

Validation of ZMYND8 as a New Treatment Target in Hepatocellular Carcinoma

Sangjoon Choi

Samsung Medical Center

Keun-Woo Lee

Samsung Medical Center

Hyun Hee Koh

Samsung Medical Center

Sujin Park

Samsung Medical Center

So-Young Yeo

Samsung Medical Center

Jae-Won Joh

Samsung Medical Center

Moon Seok Choi

Samsung Medical Center

Seok-Hyung Kim

Samsung Medical Center

Cheol-Keun Park

Seegene Medical Foundation

Sang Yun Ha (✉ sangyun.ha@skku.edu)

Samsung Medical Center <https://orcid.org/0000-0002-7346-6974>

Research Article

Keywords: Hepatocellular carcinoma, Prognosis, ZMYND8, RACK7, Target, HIF1

Posted Date: May 11th, 2021

DOI: <https://doi.org/10.21203/rs.3.rs-500308/v1>

License:  This work is licensed under a Creative Commons Attribution 4.0 International License. [Read Full License](#)

Abstract

Background: *ZMYND8* (zinc finger MYND (Myeloid, Nervy and DEAF-1)-type containing 8) has been known to play an important role in tumor regulation in various types of cancer. However, the results of *ZMYND8* expression and their clinical significance in hepatocellular carcinoma (HCC) have not yet been published. In the present study, we investigate the expression of *ZMYND8* protein and mRNA in HCC and elucidate its prognostic significance.

Methods: *ZMYND8* protein and mRNA expression in 283 and 234 HCCs were investigated using immunohistochemistry and quantitative real-time polymerase chain reactions. The relationships between *ZMYND8* expression with clinicopathologic features and prognosis of HCC patients were evaluated. Furthermore, we performed the invasion, migration, apoptosis, soft agar formation assay and sphere formation assay in HCC cell lines, and evaluated tumorigenicity in a nude mouse model, after *ZMYND8* knockdown.

Results: Overexpression of *ZMYND8* protein and mRNA was observed in 20.5% and 26.9% of HCC cases, respectively. High *ZMYND8* expression showed significant correlations with microvascular invasion, high Edmondson grade, advanced American Joint Committee on Cancer (AJCC), and increased alpha-fetoprotein level. *ZMYND8* mRNA overexpression was an independent prognostic factor for predicting early recurrence as well as short recurrence-free survival (RFS). Downregulation of *ZMYND8* reduced migration and invasion of HCC cells, and promoted apoptosis of HCC cells in an in vitro model. In a xenograft nude mouse model, knockdown of *ZMYND8* significantly reduced tumor growth.

Conclusions: *ZMYND8* mRNA overexpression could be a prognostic marker of shorter RFS in HCC patients after curative resection. *ZMYND8* might play an important role in the proliferation and progression of HCC and could be a promising candidate for targeted therapy.

Introduction

Hepatocellular carcinoma (HCC) is the most common liver malignancy and remains the fourth leading cause of cancer-related death worldwide (Bray et al. 2018). Although surgical resection is the treatment of choice in HCC, prognosis after hepatectomy is unsatisfactory because of the high incidence of tumor recurrence (Sherman 2008). Thus, it is important to predict and evaluate the risk of recurrence, and prevention with appropriate therapy is crucial to improve patient outcome (Portolani et al. 2006). Recently, several targeted therapeutics other than sorafenib have been discovered for advanced HCC, including tyrosine kinase inhibitors such as regorafenib and levatinib (Bruix et al. 2017; Kudo et al. 2018). Additionally, programmed cell death protein-1 immune checkpoint inhibitors such as nivolumab and pembrolizumab have recently been approved by the FDA, providing additional options for physicians and patients. However, application of these targeted therapies remains limited (El-Khoueiry et al. 2017; Zhu et al. 2018). In the era of precision cancer therapy, identification of reliable molecular markers and target agents is urgently needed to improve the clinical outcomes of HCC patients (Qin and Tang 2004).

ZMYND8 (zinc finger MYND (Myeloid, Nervy and DEAF-1)-type containing 8), which was first introduced as an activated protein-kinase-C-binding protein (Fossey et al. 2000), has recently been shown to play an important role as a chromatin factor in cancer biology (Gong and Miller 2018). *ZMYND8* has been reported as a tumor suppressor that works in conjunction with the H3K4me3- specific KDM5 family, such as KDM5C, in breast cancer and prostate cancer (Li et al. 2016; Shen et al. 2016). However, upregulation of *ZMYND8* by hypoxia inducible factor (HIF) or overexpression of *ZMYND8* via positive feedback of the estrogen receptor (ER) pathway was also correlated with poor prognosis of patients in breast cancer (Chen et al. 2018b; Yu et al. 2017). Immunohistochemical expression of *ZMYND8* showed favorable prognostic effects in nasopharyngeal cancers, but adverse effects in colorectal cancers (Chen et al. 2020; Chen et al. 2019). As above, it is not conclusive for the role of *ZMYND8* in cancer progression, and there have been no previous reports evaluating the role of *ZMYND8* in HCC.

In this study, we investigated the expression of *ZMYND8* in HCC according to protein and mRNA level and evaluated its association with clinicopathologic parameters and prognostic effects. Further, we performed in vitro and in vivo experiments to evaluate the role of *ZMYND8* expression in the progression of HCC.

Materials And Methods

Patients and specimens

This study included 283 patients who had Child-Pugh A liver function and underwent curative hepatectomy as a first treatment for primary HCC between July 2000 and May 2006 at Samsung Medical Center, Seoul, Korea. The definition of curative resection was a complete resection of all tumor nodules with no involvement of microscopic resection margins and no visible tumor on computed tomography at 1 month after resection. This study was approved by the Institutional Review Board of Samsung Medical Center with waiver of informed consent (IRB No. 2016-11-112, approved date: 9. 12. 2016).

Patients' electronic medical records were reviewed to obtain the clinical parameters including age, sex, time of surgery, serum α -fetoprotein (AFP) and albumin level. Histopathologic characteristics of HCCs, as well as tumor differentiation, microvascular invasion, major branch of portal vein invasion, multicentric occurrence, intrahepatic metastasis and background non-tumor liver pathology, were determined by reviewing hematoxylin and eosin-stained slides. HCC differentiation was determined using the criteria of Edmondson-Steiner grading system (Edmondson and Steiner 1954). The mitotic index, which was evaluated in a previous study, was used. Briefly, the number of mitotic cells of the tumor was added up in 10 high-power fields (HPFs) of representative whole-section slides stained with hematoxylin and eosin. High mitotic index was defined when 5 or more mitosis events were observed in 10 HPFs (Ha et al. 2016). Multicentric occurrence and intrahepatic metastasis were determined following the criteria of the Liver Cancer Study Group of Japan (Liver Cancer Study Group of Japan 2003). The recurrence of HCC within the first two years is mostly results from intrahepatic metastasis, while late recurrence mainly due to multicentric occurrence (Shimada et al. 2001). Two-years cutoff were used to classify tumor recurrence as either early or late (Imamura et al. 2003). Patients were staged according to the American Joint Committee on Cancer (AJCC) staging manual 7th edition (Edge et al. 2010) and Barcelona Clinic Liver Cancer (BCLC) staging system (Llovet et al. 1999).

Computed tomography and serum AFP were performed every 3 months in all patients after surgery. Magnetic resonance imaging was performed when tumor recurrence was suspected. The follow-up period ranged from 14 to 151.4 months (median, 119.8 months). Recurrence-free survival (RFS) was determined by the difference between the dates of surgery and intra- or extra-hepatic recurrence. Disease-specific survival (DSS) was determined as the difference between the date of surgery and the date of death associated with hepatocellular carcinoma, which was defined as the following clinical outcomes (Hoshida et al. 2008): 1. tumor occupies more than 80% of the liver; 2. tumor in the proximal part of the second branch; 3. tumor occlusion resulting in jaundice; 4. hepatic metastasis; and 5. variceal bleeding due to tumor in the proximal part of the first branch.

Immunohistochemistry

Immunohistochemistry for ZMYND8 was performed on tissue microarray blocks consisting of two 2 mm cores of HCC tissues from each case. After antigen retrieval using ER2 buffer (pH 8.0) at 100 °C for 20 minutes, The samples were incubated with primary antibody for ZMYND8 (1:200, HPA 020949, Sigma-Aldrich Inc., St.Louis, MO, USA) for 15 minutes, using a Bond-max automated immunostainer (Leica Biosystem, Melbourne, Australia). Chromogenic reactions for antigen-antibody complex were conducted for 10 min and visualized using Bond™ Polymer refine detection, DS9800 (Vision Biosystems, Melbourne, Australia). Normal brain tissue was used as a positive control. For evaluation of immunohistochemistry (IHC) of ZMYND8, the 12-point Remmele scoring system (score: 0–12) was used as described (Cho et al. 2019; Remmele and Stegner 1987). Briefly, the intensity of staining was scored on a 0 to 3 scale, and the proportion of positive tumor cells was scored from 0 to 4. The intensity and the proportion values were then multiplied, with a maximum of 12.

mRNA expression of ZMYND8 and gene set enrichment assay

We used microarray gene expression profiling data from a previously reported study by our group in the same cohort as with this study (Lim et al. 2013). The data were deposited in Gene Expression Omnibus (GSE 36376, <http://www.ncbi.nlm.nih.gov/geo/>). This dataset consists of 240 HCC tissue and 193 adjacent non-tumor liver tissues. Among them, data from 234 HCC samples and 178 non-tumor liver samples were used for this study. The normalized values of *ZMYND8* (probe ID: ILMN_2386179) expression with base 2 logarithm were extracted. In order to perform a systematic and comprehensive analysis of the characteristics of *ZMYND8* related gene sets in HCC, differentially expressed genes (DEGs) between high and low expression groups of *ZMYND8* were extracted using the Benjamini & Hochberg correction, and significant DEGs were identified as those with False Discovery Rate (FDR) q value < 0.001 . Testing for gene set enrichment of DEGs was performed using the MSigDB (<http://www.broad.mit.edu/gsea/msigdb/index.jsp>) (Mootha et al. 2003; Subramanian et al. 2005).

The Cancer Genome Atlas (TCGA) data analysis

To evaluate the prognostic significance of *ZMYND8* mRNA expression, TCGA RNA-seq data were investigated using the Gene Expression Profiling Interactive Analysis (GEPIA) dataset (<https://gepia.cancer-pku.cn/>) (Tang et al. 2017). High expression group was defined as 4th quartile in Transcripts Per Million (TPM).

Cell culture

Human liver cancer cell lines (Huh7, SNU449 and PLC/PRF5) were purchased from the Korean Cell Line Bank at December 2017, with authentication by short tandem repeat profiling. SNU449 cells were cultured in RPMI1640 (GIBCO BRL, Grand Island, NY, USA) containing 10% fetal bovine serum (GIBCO BRL), 100 mg/mL streptomycin, and 100 IU/mL penicillin at 37°C, 5% CO₂ condition. Huh7 and PLC/PRF5 were cultured in high glucose DMEM (Life Technologies, Grand Island, NY, USA) in the presence of 10% heat-inactivated fetal bovine serum (Life Technologies), 50 µg/mL streptomycin, and 100 mg/mL penicillin G (Life Technologies) at 37°C with 5% CO₂ under humidified atmosphere.

Lentivirus transduction

Human embryonic kidney 293T cells were used to produce lentivirus. Vector packaging was obtained by transfection of 293T. The cancer cells were transduced with lentivirus expressing human pLKO.1 ShNs.puro control vector, pLKO.1 ShZMYND8-1.puro and pLKO.1 shZMYND8-2.puro vectors.

Short hairpin RNA(shRNA) sequences were encoded in a DNA fragment and inserted into the pLKO.1 vector to construct the following ZMYND8 knockdown plasmids : ShZMYND8-1.puro and ShZMYND8-2.puro. Publicly available MISSION shRNA library provided by Sigma-Aldrich was used to design specific shRNAs. The ShRNA sequence is as follows:

ShZMYND8-1.puro CCGGCCTGGGTTCCAATAAATAATTCTCGAGAATTATTTATTGGAACCCAGGTTTTTG

ShZMYND8-2.puro CCGGTTGCCAATACTTCTCAGTTTCTCGAGAACTGAGGAAGTATTGGCAATTTTTG

After viral transduction, selection with 1µg/ml puromycin was performed in transduced cells. The plasmids were verified via sequencing, and their efficacies were assessed by western blotting analysis and qRT-PCR.

RNA extraction and quantitative real-time RT-PCR

Total RNA was isolated using RNease kits (#74104, Qiagen), and cDNA was synthesized with a high-capacity cDNA reverse transcription kit (#4368813, Applied Biosystems). Quantitative Real-time RT-PCR was conducted using the ABI 7900 HT Fast Real Time PCR system (Applied Biosystems, Foster City, CA) as previously described (Yeo et al. 2018). The primer sequences of ZMYND8 were as follows : The forward primer was GGGTTTATCACGCTAAGTGTCTG, and the reverse primer was GGCTTTACTCTGGGTCTCGATG.

Western blotting analysis

Cells were lysed by a RIPA lysis buffer containing 50 mM Tris pH 7.4, 150 mM NaCl, 1 mM EDTA, 1% Triton x-100, 1% Na-Doc, 0.1% SDS and protease inhibitor cocktail (Roche), and BCA protein assay kit (Thermo) was used for quantification of cell extracts. Immunoblotting was performed with ZMYND8 (Origene, TA590385, 1:1000, Rockville, MD, USA) and α-tubulin (Santa Cruz, TU-02, 1:3000, Dallas, TX) and the blots were detected with ECL reagent (#1705061, Bio-Rad).

Invasion/migration assays

In cell invasion assay, 6.5 mm Costar Transwell chambers with 8.0 µm pore size (Corning, NY, USA) were used. Appropriate Matrigel solution (1 mg/ml; Becton Dickinson, Franklin Lakes, NJ, USA) was added to the transwell filters and solidified in a 37°C incubator. Cells (1x10⁵) were planted onto the Matrigel coating. The cells on the lower surface of the Matrigel-coated filter were stained with hematoxylin and eosin after methanol fixation. The migration assay was performed in the same manner as the invasion assay except that Matrigel coating was not used.

Soft agar colony formation assay

Cells were seeded at a density of 2x10⁴ cells in 24-well culture plate, coated with 500 µl of solidified bottom agar mixture (DMEM, 10% FBS, 0.8% agar) and 500µl of top agar-medium mixture (DMEM, 10%FBS, 0.4% agar) and were incubated at 37°C. After 1 month, colonies were dyed with 0.05% Crystal Violet and the numbers were counted.

Sphere forming assay

Cells were grown in modified DMEM/F-12 containing B27 (Invitrogen, Carlsbad, CA, USA), 10 ng/mL EGF, and bFGF (Invitrogen, Carlsbad, CA, USA) in low-attachment 6 well plate (Corning Inc., Corning, NY, USA) at a density of 1x10⁴ cells/well. The medium was replaced every 2 days and the number of spheres were counted after about 14 days of incubation.

Apoptosis assay

Annexin V apoptosis detection kits (Bio-Vision, SF) was used to quantify cells apoptosis according to the manufacturer's instruction. Cells were stained with FITC-conjugated annexin-V in the dark at room temperature and were suspended in a 1X binding buffer. Cells were measured by a flow cytometer (BD Biosciences).

Xenograft

Four-week old female Balb/c nude mice (Orient Bio, Korea) were inoculated subcutaneously into the right flank with Huh7 cells (5×10^6), which were transfected with lentiviral vector expressing non-specific shRNA (shNS) or ZMYND8 shRNA (shZMYND8) and suspended in 100 μ l Matrigel/Serum-free medium (1:1 mixture). Tumor volumes were evaluated every week by a digital caliper and the volumes were calculated using the formula: length x width² x 1/2. All animal experiments approved by the Institutional Animal Care and Use Committee of Laboratory Animal Research Center at the Samsung Biomedical Research Institute

Statistical analysis

We used the X-tile statistics software (Yale University, New Haven, CT, USA) (Camp et al. 2004) to determine the optimal cut-off value of ZMYND8 protein and mRNA expression with the most significant difference in RFS. The relationships between ZMYND8 expression and clinicopathologic parameters were analyzed using chi-square test or Fisher's exact test. The Mann-Whitney U test was used for comparing differences of ZMYND8 mRNA expression between tumor and normal tissues, and mitotic index according to ZMYND8 expression status. The correlation between IHC and mRNA expression of ZMYND8 were evaluated using the spearman analysis. The Kaplan-Meier method was performed to construct survival curves. Differences in survival were evaluated using the log-rank method or Breslow test. The Cox regression analysis was performed to assess the factors which were independently associated with survival. P-values less than 0.05 (two-sided) were considered statistically significant. The SPSS software was used for statistical analysis (SPSS Inc., Chicago, IL, USA).

Results

Patient characteristics

The clinical characteristics of 283 HCC patients in the present study are summarized in Table 1. The mean age was 52.3 years (range, 17 to 76 years), 235 patients were male and 48 female. Two hundred and fifteen patients (75.8%) were infected with hepatitis B virus and 26 (9.2%) with hepatitis C virus. No viral marker was detected in 38 patients (13.4%). About 83% of patients had AJCC T stage 1 or 2 disease. The mean tumor size was 4.8 cm, and 95 (33.6%) tumors were greater than 5.0cm in size. Microvascular invasion, major portal invasion, intrahepatic metastasis, and multicentric occurrence were observed in 54.1%, 4.0%, 22.6%, and 6.0% of patients, respectively. Tumor recurrence developed in 188 (66.4%) patients, 138 (48.8%) in early recurrence and 50 (17.7%) in late recurrence. Approximately 50% of patients had background liver cirrhosis.

Table 1
The association between ZMYND8 expression and clinicopathologic parameters.

	ZMYND8 expression				ZMYND8 mRNA expression			
	No.	Low	High	p value	No.	Low	High	p value
	n = 283	n = 225 (%)	n = 58 (%)		n = 234	n = 171 (%)	n = 63 (%)	
Age, year								
≤ 55	164	126 (56.0)	38 (65.5)	0.190	136	100 (58.5)	36 (57.1)	0.854
> 55	119	99 (44.0)	20 (34.5)		98	71 (41.5)	27 (42.9)	
Gender								
Female	48	38 (16.9)	10 (17.2)	0.949	38	31 (18.1)	7 (11.1)	0.197
Male	235	187 (83.1)	48 (82.8)		196	140 (81.9)	56 (88.9)	
Tumor size, cm								
≤ 5.0	188	155 (68.9)	33 (56.9)	0.085	155	124 (72.5)	31 (49.2)	0.001
> 5.0	95	70 (31.1)	25 (43.1)		79	47 (27.5)	32 (50.8)	
Edmondson grade								
I	32	28 (12.4)	4 (6.9)	< 0.001	24	21 (12.3)	3 (4.8)	0.018
II	227	187 (83.1)	40 (69.0)		190	140 (81.9)	50 (79.4)	
III	24	10 (4.4)	14 (24.1)		20	10 (5.8)	10 (15.9)	
Microvascular invasion								
(-)	130	118 (52.4)	12 (20.7)	< 0.001	105	89 (52.0)	16 (25.4)	< 0.001
(+)	153	107 (47.6)	46 (79.3)		129	82 (48.0)	47 (74.6)	
Major portal vein invasion								
(-)	272	218 (96.9)	54 (93.1)	0.245	225	166 (97.1)	59 (93.7)	0.256 ^{b)}
(+)	11	7 (3.1)	4 (6.9)		9	5 (2.9)	4 (6.3)	
Intrahepatic metastasis								
(-)	219	182 (80.9)	37 (63.8)	0.006	181	136 (79.5)	45 (71.4)	0.189
(+)	64	43 (19.1)	21 (36.2)		53	35 (20.6)	18 (28.6)	
Multicentric occurrence								
(-)	266	209 (92.9)	57 (98.3)	0.211	222	161 (94.2)	61 (96.8)	0.522 ^{b)}
(+)	17	16 (7.1)	1 (1.7)		12	10 (5.8)	2 (3.2)	
Mitotic index								
Low (≤ 4/10 HPF)	155	148 (65.8)	7 (12.1)	< 0.001	128	105 (61.4)	23 (36.5)	0.001
High (≥ 5/10 HPF)	128	77 (34.2)	51 (87.9)		106	66 (38.6)	40 (63.5)	
Tumor necrosis								
(-)	215	188 (83.6)	27 (46.6)	< 0.001	176	141 (82.5)	35 (55.6)	< 0.001
(+)	68	37 (16.4)	31 (53.4)		58	30 (17.5)	28 (44.4)	
AJCC T-stage ^{b)}								

	ZMYND8 expression				ZMYND8 mRNA expression			
1	122	110 (48.9)	12 (20.7)	< 0.001	100	85 (49.7)	15 (23.8)	0.002 ^{b)}
2	113	83 (36.9)	30 (51.7)		96	60 (35.1)	36 (57.1)	
3	42	28 (12.4)	14 (24.1)		33	22 (12.9)	11 (17.5)	
4	6	4 (1.8)	2 (3.4)		5	4 (2.3)	1 (1.6)	
BCLC stage								
0-A	163	134 (59.6)	29 (50.0)	0.347	135	110 (64.3)	25 (39.7)	0.003
B	107	82 (36.4)	25 (43.1)		89	55 (32.2)	34 (54.0)	
C	13	9 (4.0)	4 (6.9)		10	6 (3.5)	4 (6.3)	
Albumin level, g/dL								
> 3.5	28	206 (91.6)	49 (84.5)	0.108	22	157 (91.8)	55 (87.3)	0.294
≤ 3.5	255	19 (8.4)	9 (15.5)		212	14 (8.2)	8 (12.7)	
AFP level, ng/mL ^{a)}								
≤ 200	173	148 (68.5)	25 (43.9)	0.001	145	115 (69.7)	30 (48.4)	0.003
> 200	100	68 (31.5)	32 (56.1)		82	50 (30.3)	32 (51.6)	
Etiology								
Non-viral	38	29 (12.9)	9 (15.5)	0.526	32	23 (13.5)	9 (14.3)	0.985 ^{b)}
HBV	215	173 (76.9)	42 (72.4)		179	131 (76.6)	48 (76.2)	
HCV	26	20 (8.9)	6 (10.3)		20	15 (8.8)	5 (7.9)	
HBV & HCV	4	3 (1.3)	1 (1.7)		3	2 (1.2)	1 (1.6)	
Liver cirrhosis								
(-)	140	115 (51.1)	25 (43.1)	0.277	120	87 (50.9)	33 (52.4)	0.838
(+)	143	110 (48.9)	33 (56.9)		114	84 (49.1)	30 (47.6)	
Early recurrence								
(≤ 2 years)								
(-) ^{c)}	145	120 (53.3)	25 (43.1)	0.165	124	99 (58.2)	25 (39.1)	0.013
(+)	138	105 (46.7)	33 (56.9)		110	72 (42.1)	38 (60.3)	
Late recurrence								
(> 2 years)								
(-) ^{c)}	95	78 (65.0)	17 (68.0)	0.774	83	66 (66.7)	17 (68.0)	0.899
(+)	50	42 (35.0)	8 (32.0)		41	33 (33.3)	8 (32.0)	
AJCC, American Joint Committee on Cancer; BCLC, Barcelona Clinic Liver Cancer; AFP, α-fetoprotein; HBV, hepatitis B virus; HCV, hepatitis C virus.								
^{a)} AFP evaluation was not applicable in 10 cases., ^{b)} by Fisher's exact test, otherwise by chi-square test, ^{c)} No early or late recurrence								

In HCC, immunoreactivity for ZMYND8 was observed in the nucleus of tumor cells (Fig. 1). No immunoreactivity was detected in background non-tumor hepatocytes. The mean IHC expression Remmele score of ZMYND8 was 1.86 (median, 0, range, 0–12). ZMYND8 expression was regarded as high when the IHC score was greater than 4.0, which was determined as the best cutoff value associated with recurrence free survival (RFS) via the X-tile package. ZMYND8 protein overexpression was observed in 58 of the 283 HCC patients (20.5%). The associations between ZMYND8 protein expression and clinicopathologic characteristics are summarized in Table 1. High ZMYND8 expression was significantly associated with higher Edmondson grade ($p < 0.001$), high mitotic index ($p < 0.001$), tumor necrosis ($p < 0.001$), microvascular invasion ($p < 0.001$), intrahepatic metastasis ($p = 0.006$), advanced AJCC T stage ($p < 0.001$), and increased serum AFP level ($p = 0.001$). The mean mitotic index was significantly higher in the high ZMYND8 expression group than the low expression group (mean \pm standard deviation, 17.93 ± 14.42 vs. 5.14 ± 7.93 , $p < 0.001$).

ZMYND8 mRNA expression in HCC

The quantification of ZMYND8 mRNA expression was available in 234 HCC samples. The mean mRNA expression of ZMYND8 was 7.00 (median, 6.97, range 6.27–8.22). Expression of ZMYND8 was higher in HCC tissue than in background non-tumor tissue (mean \pm standard deviation, 7.00 ± 0.32 vs 6.68 ± 0.16 , $p < 0.001$, Fig. 2A). The spearman's correlation analysis revealed a statistically significant positive correlation between ZMYND8 protein and ZMYND8 mRNA expression level ($r = 0.354$, $p < 0.001$, Fig. 2B). The best cutoff value of ZMYND8 mRNA level with the highest level of statistical significance related to RFS was 7.12 via the X-tile package. High ZMYND8 mRNA expression was observed in 63 of the 234 HCC patients (26.9%). Table 1 summarizes the clinicopathologic parameters with ZMYND8 mRNA level. High ZMYND8 mRNA expression showed significant association with larger tumor size ($p = 0.001$), higher Edmondson grade ($p = 0.018$), high mitotic index ($p = 0.001$), tumor necrosis ($p < 0.001$), microvascular invasion ($p < 0.001$), advanced AJCC T stage ($p = 0.002$), advanced BCLC stage ($p = 0.003$), increased AFP level ($p = 0.003$), and early recurrence ($p = 0.013$). The mean mitotic index was significantly higher in the high ZMYND8 expression group than the low expression group (mean \pm standard deviation, 12.65 ± 14.33 vs. 6.09 ± 8.79 , $p < 0.001$).

Association between ZMYND8 expression and prognosis of HCC patients

The high ZMYND8 protein expression group showed a stronger trend toward shorter RFS ($p = 0.053$) and a significantly shorter disease specific survival (DSS) ($p = 0.02$) by the log rank test, as compared to the low ZMYND8 expression group according to a survival analysis with a 79.5 month mean follow-up period (Fig. 3A and 3B). By applying the Breslow test, which attributes greater weight to earlier events, patients with high ZMYND8 protein expression showed significantly shorter RFS ($p = 0.002$). Patients with high ZMYND8 mRNA expression showed a shorter RFS ($p = 0.003$) and DSS ($p = 0.037$) than those with low expression (Fig. 3C and 3D).

On univariable analysis, larger tumor size, higher Edmondson grade, tumor necrosis, microvascular invasion, major portal vein invasion, intrahepatic metastasis, higher AJCC T-stage, higher BCLC stage, lower albumin level, and high serum AFP level showed unfavorable influences on both RFS and DSS. Viral etiology unfavorably influenced RFS. A high mitotic index showed unfavorable effects on DSS. High ZMYND8 protein expression showed unfavorable effects on DSS ($p = 0.021$, hazard ratio 1.695) and high ZMYND8 mRNA expression showed unfavorable effects on both RFS ($p = 0.003$, hazard ratio 1.697) and DSS ($p = 0.039$, hazard ratio 1.640) (Table 2).

Table 2
Univariable analysis for recurrence free survival and disease-specific survival

	Recurrence free survival		Disease specific survival	
	HR (95% CI)	p value	HR (95% CI)	p value
Age, year				
> 55 vs ≤ 55	0.968 (0.723–1.297)	0.829	0.936 (0.625–1.400)	0.747
Gender				
Male vs Female	0.979 (0.675–1.419)	0.910	0.910 (0.696–1.189)	0.488
Tumor size, cm				
> 5.0 vs ≤ 5.0	1.757 (1.309–2.358)	< 0.001	2.930 (1.969–4.360)	< 0.001
Edmondson grade				
III vs I, II	2.242 (1.421–3.539)	0.001	2.670 (1.514–4.710)	0.001
Microvascular invasion				
(+) vs (-)	2.210 (1.644–2.971)	< 0.001	3.225 (2.057–5.056)	< 0.001
Major portal vein invasion				
(+) vs (-)	3.420 (1.802–6.493)	< 0.001	5.024 (2.518–10.024)	< 0.001
Intrahepatic metastasis				
(+) vs (-)	4.980 (3.593–6.903)	< 0.001	5.838 (3.890–8.760)	< 0.001
Multicentric occurrence				
(+) vs (-)	1.183 (0.625–2.241)	0.605	0.669 (0.246–1.821)	0.432
Mitotic index				
High vs Low	1.293 (0.971–1.722)	0.079	2.126 (1.422–3.177)	< 0.001
Tumor necrosis				
(+) vs (-)	2.610 (1.899–3.585)	< 0.001	4.345 (2.909–6.492)	< 0.001
AJCC T-stage				
2,3,4 vs 1	2.256 (1.672–3.044)	< 0.001	3.265 (2.058–5.181)	< 0.001
BCLC stage				
B,C vs 0, A	2.141 (1.605–2.855)	< 0.001	3.970 (2.606–6.046)	< 0.001
Albumin level, g/dL				
≤ 3.5 vs > 3.5	1.859 (1.190–2.905)	0.006	2.367 (1.362–4.115)	0.002
AFP level, ng/mL ^{a)}				
> 200 vs ≤ 200	1.721 (1.283–2.310)	< 0.001	1.772 (1.181–2.658)	0.006
Etiology				
Viral vs Non-viral	2.032 (1.233–3.348)	0.005	1.526 (0.793–2.935)	0.206
Liver cirrhosis				
(+) vs (-)	1.314 (0.986–1.752)	0.062	1.031 (0.694–1.531)	0.882

HR, Hazard Ratio; CI, Confidence Interval; AJCC, American Joint Committee on Cancer; BCLC, Barcelona Clinic Liver Cancer; IHC, Immunohistochemistry

	Recurrence free survival		Disease specific survival	
ZMYND8 expression (IHC)				
High vs Low	1.406 (0.994–1.988)	0.054	1.695 (1.082–2.654)	0.021
ZMYND8 expression (mRNA)				
High vs Low	1.697 (1.198–2.405)	0.003	1.640 (1.026–2.620)	0.039
HR, Hazard Ratio; CI, Confidence Interval; AJCC, American Joint Committee on Cancer; BCLC, Barcelona Clinic Liver Cancer; IHC, Immunohistochemistry				

We classified ZMYND8 expression as mRNA and protein and performed multivariable analysis two times with each variable. Multivariable analysis with ZMYND8 protein expression showed that intrahepatic metastasis and tumor necrosis were independent predictors of both shorter RFS and shorter DSS, and low AFP level was an independent predictor for shorter DSS. ZMYND8 protein overexpression was not an independent prognostic factor for RFS or DSS (Table 3). On multivariable analysis with *ZMYND8* mRNA expression, intrahepatic metastasis and tumor necrosis were found to be an independent predictor of both shorter RFS and DSS. *ZMYND8* mRNA expression was an independent predictor for RFS ($p = 0.020$, hazard ratio 1.572), not for DSS ($p = 0.864$) (Table 4).

Table 3
Multivariable analysis for recurrence free survival and disease-specific survival including ZMYND8 protein expression

	Recurrence free survival		Disease specific survival	
	HR (95% CI)	p value	HR (95% CI)	p value
Tumor size, cm				
> 5.0 vs ≤ 5.0	0.934 (0.657–1.330)	0.707	1.504 (0.0921–2.458)	0.103
Edmondson grade				
III vs I, II	1.359 (0.813–2.271)	0.241	0.979 (0.508–1.887)	0.949
Microvascular invasion				
(+) vs (-)	1.056 (0.687–1.624)	0.804	0.715 (0.369–1.385)	0.320
Major portal vein invasion				
(+) vs (-)	0.796 (0.382–1.657)	0.542	1.180 (0.545–2.555)	0.674
Intrahepatic metastasis				
(+) vs (-)	4.492 (2.896–6.967)	< 0.001	4.962 (2.840–8.670)	< 0.001
Mitotic index				
High vs Low	0.727 (0.507–1.042)	0.083	1.449 (0.879–2.389)	0.145
Tumor necrosis				
(+) vs (-)	2.302 (1.502–3.527)	< 0.001	3.609 (2.122–6.138)	< 0.001
Albumin level, g/dL				
≤ 3.5 vs > 3.5	1.363 (0.817–2.277)	0.236	1.372 (0.720–2.616)	0.336
AFP level, ng/mL ^{a)}				
> 200 vs ≤ 200	1.393 (1.008–1.925)	0.044	1.148 (0.718–1.836)	0.565
Etiology				
Viral vs Non-viral	1.515 (0.894–2.565)	0.122	0.962 (0.471–1.962)	0.915
ZMYND8 expression (IHC)				
High vs Low	0.898 (0.585–1.377)	0.621	0.735 (0.419–1.288)	0.282
HR, Hazard Ratio; CI, Confidence Interval; IHC, Immunohistochemistry				

Table 4
Multivariable analysis for recurrence free survival and disease-specific survival including *ZMYND8* mRNA expression

	Recurrence free survival		Disease specific survival	
	HR (95% CI)	p value	HR (95% CI)	p value
Tumor size, cm				
> 5.0 vs ≤ 5.0	0.793 (0.539–1.167)	0.240	1.470 (0.854–2.530)	0.165
Edmondson grade				
III vs I, II	1.469 (0.821–2.630)	0.195	0.808 (0.387–1.689)	0.571
Microvascular invasion				
(+) vs (-)	1.032 (0.634–1.681)	0.898	0.656 (0.308–1.398)	0.275
Major portal vein invasion				
(+) vs (-)	0.679 (0.299–1.542)	0.355	1.583 (0.682–3.676)	0.285
Intrahepatic metastasis				
(+) vs (-)	5.854 (3.572–9.594)	< 0.001	4.758 (2.576–8.788)	< 0.001
Mitotic index				
High vs Low	0.673 (0.452–1.002)	0.051	1.470 (0.844–2.561)	0.174
Tumor necrosis				
(+) vs (-)	2.064 (1.326–3.215)	0.001	3.473 (1.957–6.164)	< 0.001
Albumin level, g/dL				
≤ 3.5 vs > 3.5	1.207 (0.691–2.109)	0.509	1.208 (0.599–2.437)	0.597
AFP level, ng/mL ^{a)}				
> 200 vs ≤ 200	1.257 (0.871–1.813)	0.222	1.029 (0.615–1.724)	0.913
Etiology				
Viral vs Non-viral	1.699 (0.931–3.103)	0.084	1.020 (0.458–2.272)	0.961
<i>ZMYND8</i> expression (mRNA)				
High vs Low	1.572 (1.074–2.300)	0.020	1.047 (0.622–1.761)	0.864
HR, Hazard Ratio; CI, Confidence Interval				

Prognostic effect of *ZMYND8* mRNA expression in TCGA data

We found the unfavorable prognostic effect of *ZMYND8* expression in an independent HCC cohort consisting of TCGA RNAseq samples. Patients with high expression of *ZMYND8* mRNA showed shorter RFS ($p = 0.008$) and OS ($p = 0.003$) than those with low expression ($p < 0.001$) (Fig. 3E and 3F).

Gene set enrichment analysis in *ZMYND8*-high HCC

List of DEGs between high and low expression group of *ZMYND8* was summarized in supplementary Table 1, and list of significantly enriched gene sets according to *ZMYND8* expression status was summarized in Table 5. Gene signatures related to cell proliferation were significantly enriched, including gene sets of E2F targets, G2M checkpoint, MYC targets, mitotic spindle and apoptosis. In addition, the expression of *ZMYND8* was strongly associated with the enrichment of gene sets involved in hypoxia, oxidative phosphorylation and angiogenesis, as well as apical junction and epithelial-mesenchymal transition. Gene set of DNA repair was also significantly enriched.

Table 5
List of enriched gene sets according to ZMYND8 expression status in hepatocellular carcinomas.

Gene Set Name	# Genes in Gene Set (K)	Description	# Genes in Overlap (k)	k/K	p-value	FDR q-value
HALLMARK_E2F_TARGETS	200	Genes encoding cell cycle related targets of E2F transcription factors.	58	0.29	1.44E-43	7.19E-42
HALLMARK_G2M_CHECKPOINT	200	Genes involved in the G2/M checkpoint, as in progression through the cell division cycle.	47	0.235	5.62E-31	1.41E-29
HALLMARK_COAGULATION	138	Genes encoding components of blood coagulation system; also up-regulated in platelets.	37	0.2681	6.92E-27	1.15E-25
HALLMARK_XENOBIOTIC_METABOLISM	200	Genes encoding proteins involved in processing of drugs and other xenobiotics.	43	0.215	9.30E-27	1.16E-25
HALLMARK_MYC_TARGETS_V1	200	A subgroup of genes regulated by MYC - version 1 (v1).	41	0.205	9.99E-25	9.99E-24
HALLMARK_MYC_TARGETS_V2	58	A subgroup of genes regulated by MYC - version 2 (v2).	18	0.3103	4.93E-15	4.11E-14
HALLMARK_FATTY_ACID_METABOLISM	158	Genes encoding proteins involved in metabolism of fatty acids.	25	0.1582	6.37E-13	4.55E-12
HALLMARK_MTORC1_SIGNALING	200	Genes up-regulated through activation of mTORC1 complex.	26	0.13	2.22E-11	1.39E-10
HALLMARK_BILE_ACID_METABOLISM	112	Genes involve in metabolism of bile acids and salts.	19	0.1696	1.07E-10	5.94E-10
HALLMARK_MITOTIC_SPINDLE	199	Genes important for mitotic spindle assembly.	23	0.1156	3.23E-09	1.61E-08
HALLMARK_PEROXISOME	104	Genes encoding components of peroxisome.	16	0.1538	1.35E-08	6.16E-08

Gene Set Name	# Genes in Gene Set (K)	Description	# Genes in Overlap (k)	k/K	p-value	FDR q-value
HALLMARK_COMPLEMENT	200	Genes encoding components of the complement system, which is part of the innate immune system.	21	0.105	8.26E-08	3.44E-07
HALLMARK_ADIPOGENESIS	200	Genes up-regulated during adipocyte differentiation (adipogenesis).	20	0.1	3.69E-07	1.42E-06
HALLMARK_EPITHELIAL_MESENCHYMAL_TRANSITION	200	Genes defining epithelial-mesenchymal transition, as in wound healing, fibrosis and metastasis.	18	0.09	6.24E-06	1.84E-05
HALLMARK_GLYCOLYSIS	200	Genes encoding proteins involved in glycolysis and gluconeogenesis.	18	0.09	6.24E-06	1.84E-05
HALLMARK_KRAS_SIGNALING_UP	200	Genes up-regulated by KRAS activation.	18	0.09	6.24E-06	1.84E-05
HALLMARK_OXIDATIVE_PHOSPHORYLATION	200	Genes encoding proteins involved in oxidative phosphorylation.	18	0.09	6.24E-06	1.84E-05
HALLMARK_ANDROGEN_RESPONSE	100	Genes defining response to androgens.	12	0.12	1.25E-05	3.46E-05
HALLMARK_APOPTOSIS	161	Genes mediating programmed cell death (apoptosis) by activation of caspases.	15	0.0932	2.41E-05	6.34E-05
HALLMARK_UV_RESPONSE_UP	158	Genes up-regulated in response to ultraviolet (UV) radiation.	14	0.0886	7.71E-05	1.90E-04
HALLMARK_APICAL_JUNCTION	200	Genes encoding components of apical junction complex.	16	0.08	8.36E-05	1.90E-04
HALLMARK_ESTROGEN_RESPONSE_LATE	200	Genes defining late response to estrogen.	16	0.08	8.36E-05	1.90E-04
HALLMARK_HYPOXIA	200	Genes up-regulated in response to low oxygen levels (hypoxia).	15	0.075	2.79E-04	6.06E-04

Gene Set Name	# Genes in Gene Set (K)	Description	# Genes in Overlap (k)	k/K	p-value	FDR q-value
HALLMARK_ANGIOGENESIS	36	Genes up-regulated during formation of blood vessels (angiogenesis).	6	0.1667	3.17E-04	6.61E-04
HALLMARK_DNA_REPAIR	150	Genes involved in DNA repair.	12	0.08	6.22E-04	1.24E-03
HALLMARK_UNFOLDED_PROTEIN_RESPONSE	113	Genes up-regulated during unfolded protein response, a cellular stress response related to the endoplasmic reticulum.	10	0.0885	7.97E-04	1.53E-03
HALLMARK_HEDGEHOG_SIGNALING	36	Genes up-regulated by activation of hedgehog signaling.	5	0.1389	2.35E-03	4.31E-03
HALLMARK_IL2_STAT5_SIGNALING	199	Genes up-regulated by STAT5 in response to IL2 stimulation.	13	0.0653	2.41E-03	4.31E-03
HALLMARK_MYOGENESIS	200 + B3B31:C31	Genes involved in development of skeletal muscle (myogenesis).	13	0.065	2.52E-03	4.35E-03

Table is sorted in the order of q value, and only the list of q values less than 0.005 was displayed.

ZMYND8 expression affects invasiveness and tumorigenesis of HCCs

We performed in vitro and in vivo assays to evaluate the clinical observations of *ZMYND8* mentioned above. After knockdown of *ZMYND8* with treatment of Sh-ZMYND8 in the Huh7, SNU449, PLC/PRF5 cell lines (Fig. 4A-B), sphere formation, soft agar colony formation migration and invasion of cancer cells were dramatically decreased (Fig. 4C-D). The rate of early and late apoptosis increased after Sh-ZMYND8 treatment (Fig. 4E). Downregulation of *ZMYND8* inhibited the growth of HCC xenografts in Balb/c nude mice (Fig. 4F).

Discussion

In the present study, we first demonstrated that *ZMYND8* mRNA expression was up-regulated in HCC tissues compared to background non-tumor liver tissue, and high *ZMYND8* expression by both mRNA and protein was associated with aggressive clinicopathologic parameters such as high Edmondson grade, microvascular invasion, intrahepatic metastasis, advanced AJCC T stage, and high AFP level, as well as frequent tumor necrosis and high mitotic index. Patients with high expression of *ZMYND8* showed shorter RFS and DSS in a large cohort of HCC patients with long-term follow-up. Especially, *ZMYND8* mRNA expression was an independent predictor for shorter RFS. The prognostic effect of *ZMYND8* expression was also confirmed in an independent cohort of TCGA dataset. These clinical observations were confirmed by in vitro and in vivo experiments. Knockdown of *ZMYND8* induced significant decrease in migration, invasion, and tumorigenicity on in vitro model, and suppressed the tumor growth of HCC xenografts in vivo model. These results suggest that *ZMYND8* plays a critical role in HCC progression.

ZMYND8 was initially identified as a receptor for activated C-kinase (RACK) protein that binds to an activated protein-kinase-C beta I (PKCβ1) (Fossey et al. 2000), and has been shown to play as a central chromatin factor in DNA damage response and cancer (Gong and

Miller 2018). There have been several studies regarding ZMYND8 as a tumor suppressor. ZMYND8 collaborates with H3K4me3- specific KDM5 family, such as KDM5C or KDM5D, and regulates transcription (Li et al. 2016; Shen et al. 2016). Shen et al. showed that loss of ZMYND8 or KDM5C induced enhanced cell migration and invasion, as well as tumor growth in a breast ZR-75-30 mouse xenograft model, by increasing the level of H3K4me3, subsequent enhancer RNA levels, and expression of neighboring genes such as oncogenic family of S100A proteins (Shen et al. 2016). Li et al. demonstrated that ZMYND8 and KDM5D are necessary for repressing metastasis-linked gene, and loss of these genes lead to increased cell migration and invasiveness of a prostate DU145 mouse xenograft model (Li et al. 2016). Basu et al. demonstrated *ZMYND8* as a target gene of all-*trans* retinoic acid (ATRA), involved in ATRA-mediated inhibition of cancer proliferation, and regulated epithelial to mesenchymal transition to maintain the epithelial phenotypes by selective enrichment on *CLDN1/CDH1* (Basu et al. 2017a; Basu et al. 2017b). Low expression of ZMYND8 protein by IHC have been reported as an independent prognostic factor for worse survival in nasopharyngeal carcinoma (Chen et al. 2019).

However, there have been studies reporting *ZMYND8* as an oncogenes. Kuroyanagi et al. found *ZMYND8* as one of the most significantly changed genes in the tumor angiogenesis-positive group than in the negative group, using a prostate DU145-xenografted zebrafish model, and showed that ZMYND8 promotes tumor angiogenesis and cancer cell proliferation induced by hypoxia (Kuroyanagi et al. 2014). Yu et al. showed that overexpression of ZMYND8 involved in a positive feedback circuit of the estrogen receptor pathway was more prevalent in luminal B breast cancers and associated with poor survival (Yu et al. 2017). High expression of ZMYND8 protein by IHC has been reported as an independent prognostic factor for shorter survival in colorectal cancers (Chen et al. 2020). In a recent comprehensive study by Chen et al., up-regulation of *ZMYND8* was correlated with poor survival in breast cancer. Knockdown of *ZMYND8* decreased tumor growth and lung metastasis in a hypoxia induced factor (HIF) dependent manner, by epigenetic mechanism. Specifically, Acetylation of ZMYND8 at lysine 1007 and 1034 by HIF coactivator p300 induced RNA polymerase II phosphorylation and subsequent transcriptional elongation of the HIF target genes (Chen et al. 2018b). These results highlighting oncogenic function of ZMYND8 are consistent with those of our study performed in HCC. It seems that ZMYND8 has the dual role as a tumor suppressor or promoter, and that role depends on the specific types of genes it interacts with and the types of tumors.

HCC is one of the most hypoxic tumors, and activation of hypoxia signaling pathway, including HIF and its transcriptional coactivators, mediates increased tumor cell proliferation, invasion, and metastasis. (Chen and Lou 2017). Under a hypoxia state, ZMYND8 physically interacts with HIF-1a and HIF-2a, and activates HIF transcriptional activity in breast cancer (Chen et al. 2018a; Chen et al. 2018b). Additionally, ZMYND8 is acetylated by the histone acetyltransferase p300 and promotes the HIF target gene expression (Chen et al. 2018a). Interestingly, high expression of both HIF and p300 are associated with aggressive features and poor prognosis of HCC (Li et al. 2011; Xiang et al. 2012). In the present study, high expression of ZMYND8 was significantly associated with a high mitotic index and tumor necrosis, reflecting the hypoxic state of HCC. Also, *ZMYND8* expression was significantly associated with gene set pathways associated with cell cycle, mitosis, hypoxia, and angiogenesis, supporting the results of previous studies. Recent studies have been targeting the molecules of the hypoxia pathway in HCC. Ma et al. demonstrated that 2-Methoxyestradiol, a HIF inhibitor, reduced the expression of both HIF-1a and HIF-2a as well as their downstream molecules, and consequently suppressed tumor proliferation and angiogenesis of HCC cells (Ma et al. 2014). Moreover, Inajaki et al. reported that the proliferation and invasion of HCC cells significantly reduced after p300 inhibitor treatment (Inagaki et al. 2016). Thus, we could infer that ZMYND8, which is one of the main transcription regulator complexes combined with HIF and p300 can also become potential target for novel HCC therapy.

The limitation of our study is that we could not elucidate the specific molecular mechanism of *ZMYND8* and its functional relationship with other genes. Despite the limitation, we provide valuable information about the close association between *ZMYND8* expression and clinicopathologic features in a large cohort of HCC for the first time, with relevant experimental data. Also, we could indirectly suggest that *ZMYND8* may has a crucial role on aggressive tumor behavior in HCC by interacting with genes involved in pathway such as cell cycle, mitosis, hypoxia, angiogenesis and epithelial-mesenchymal transition through gene set enrichment assay. Interestingly, DNA mismatch repair pathway was also significantly enriched. Gong et al. reported *ZMYND8* as a key chromatin modulator of the DNA damage response and DNA repair (Gong et al. 2015; Gong et al. 2017), and Wang et al. showed that upregulation of *ZMYND8* promoted tumor growth by reducing DNA damage and thereby evading cytotoxic T lymphocyte surveillance in breast cancer (Wang et al. 2020). The association between *ZMYND8* expression and genes involved in DNA mismatch repair pathway is a possible regulator of immune response and provide the insight for immunotherapy. Further study is necessary to unveil the specific mechanisms of *ZMYND8* involved in the progression of HCC.

Conclusions

We demonstrated that high expression of ZMYND8 is associated with advanced stage and poor patient survival in HCC for the first time, and knockdown of *ZMYND8* decreased invasion, migration, and proliferation in an in vitro model, as well as tumorigenesis in an in vivo xenograft model. ZMYND8 may be used as a prognostic biomarker and is a potential candidate for therapeutic targets in HCC.

Abbreviations

HCC: Hepatocellular carcinoma; ZMYND8: zinc finger MYND (Myeloid, Nervy and DEAF-1)-type containing 8; HIF: Hypoxia inducible factor; ER: Estrogen receptor; AFP: α -fetoprotein; HPFs: High power fields; AJCC: American Joint Committee on Cancer; BCLC: Barcelona Clinic Liver Cancer; RFS: Recurrence-free survival; DSS: Disease-specific survival; IHC: Immunohistochemistry; DEG: Differentially expressed genes; FDR: False Discovery Rate; TCGA: The Cancer Genome Atlas; GEPIA: Gene Expression Profiling Interactive Analysis; shRNA: Short hairpin RNA; RACK: Receptor for activated C-kinase; PKC β 1: Protein-kinase-C beta I; ATRA: all-*trans* retinoic acid

Declarations

Ethics approval and consent to participate

The Institutional Review Board of Samsung Medical Center approved this study and waived informed consent for this study.

Consent for publication

All authors agreed to publish the article.

Availability of data and materials

All datasets used and analyzed during this study are available from the corresponding author on reasonable request.

Competing interest

All contributing authors have no financial support relevant to this article and no competing interests to declare.

Funding

This study was funded by the Basic Science Research Program through the National Research Foundation of Korea (NRF) funded by the Ministry of Education (NRF-2017R1C1B5017890 and NRF-2018R1C1B6006428).

Author's contributions

SC performed data analysis, generated tables and figures, and drafted the manuscript. KWL performed in vitro and in vivo assays, analyzed the data and drafted the manuscript. HHK analyzed data. SP, SY, JWJ, MSC supported data acquisition. SHK and CKP contributed to knowledge. SYH conceptualized and designed the study, collected and analyzed the data, drafted and revised the manuscript. All authors have read and agreed to the published version of the manuscript.

Acknowledgements

Not applicable

References

1. Basu M, Khan MW, Chakrabarti P, Das C (2017a) Chromatin reader ZMYND8 is a key target of all trans retinoic acid-mediated inhibition of cancer cell proliferation. *Biochim Biophys Acta Gene Regul Mech* 1860:450-459. <https://doi.org/10.1016/j.bbagr.2017.02.004>
2. Basu M, Sengupta I, Khan MW, Srivastava DK, Chakrabarti P, Roy S, Das C (2017b) Dual histone reader ZMYND8 inhibits cancer cell invasion by positively regulating epithelial genes. *Biochem J* 474:1919-1934. <https://doi.org/10.1042/bcj20170223>
3. Bray F, Ferlay J, Soerjomataram I, Siegel RL, Torre LA, Jemal A (2018) Global cancer statistics 2018: GLOBOCAN estimates of incidence and mortality worldwide for 36 cancers in 185 countries. *CA: a cancer journal for clinicians* 68:394-424

4. Bruix J, Qin S, Merle P, Granito A, Huang Y-H, Bodoky G, Pracht M, Yokosuka O, Rosmorduc O, Breder V, Gerolami R, Masi G, Ross PJ, Song T, Bronowicki J-P, Ollivier-Hourmand I, Kudo M, Cheng A-L, Llovet JM, Finn RS, LeBerre M-A, Baumhauer A, Meinhardt G, Han G (2017) Regorafenib for patients with hepatocellular carcinoma who progressed on sorafenib treatment (RESORCE): a randomised, double-blind, placebo-controlled, phase 3 trial. *The Lancet* 389:56-66. [https://doi.org/10.1016/s0140-6736\(16\)32453-9](https://doi.org/10.1016/s0140-6736(16)32453-9)
5. Camp RL, Dolled-Filhart M, Rimm DL (2004) X-Tile. A New Bio-Informatics Tool for Biomarker Assessment and Outcome-Based Cut-Point Optimization 10:7252-7259. <https://doi.org/10.1158/1078-0432.Ccr-04-0713>
6. Chen C, Lou T (2017) Hypoxia inducible factors in hepatocellular carcinoma. *Oncotarget* 8:46691-46703. <https://doi.org/10.18632/oncotarget.17358>
7. Chen J, He Q, Wu P, Fu J, Xiao Y, Chen K, Xie D, Zhang X (2020) ZMYND8 expression combined with pN and pM classification as a novel prognostic prediction model for colorectal cancer: Based on TCGA and GEO database analysis. *Cancer Biomark* 28:201-211. <https://doi.org/10.3233/cbm-191261>
8. Chen J, Liu J, Chen X, Li Y, Li Z, Shen C, Chen K, Zhang X (2019) Low expression of ZMYND8 correlates with aggressive features and poor prognosis in nasopharyngeal carcinoma. *Cancer Manag Res* 11:7835-7843. <https://doi.org/10.2147/cmar.S210305>
9. Chen Y, Wang Y, Luo W (2018a) ZMYND8 is a primary HIF coactivator that mediates breast cancer progression. *Mol Cell Oncol* 5:e1479619. <https://doi.org/10.1080/23723556.2018.1479619>
10. Chen Y, Zhang B, Bao L, Jin L, Yang M, Peng Y, Kumar A, Wang JE, Wang C, Zou X, Xing C, Wang Y, Luo W (2018b) ZMYND8 acetylation mediates HIF-dependent breast cancer progression and metastasis. *J Clin Invest* 128:1937-1955. <https://doi.org/10.1172/jci95089>
11. Cho J, Kim KM, Kim HC, Lee WY, Kang WK, Park YS, Ha SY (2019) The prognostic role of tumor associated glycoprotein 72 (TAG-72) in stage II and III colorectal adenocarcinoma. *Pathol Res Pract* 215:171-176. <https://doi.org/10.1016/j.prp.2018.10.024>
12. Edge S, Byrd D, Compton C, Fritz A, Greene F, Trotti IA (2010) *AJCC cancer staging manual*, 7th edn. Springer, Chicago, IL
13. Edmondson H, Steiner P (1954) Primary carcinoma of the liver: a study of 100 cases among 48,900 necropsies. *Cancer* 7:462-503
14. El-Khoueiry AB, Sangro B, Yau T, Crocenzi TS, Kudo M, Hsu C, Kim T-Y, Choo S-P, Trojan J, Welling TH, Meyer T, Kang Y-K, Yeo W, Chopra A, Anderson J, dela Cruz C, Lang L, Neely J, Tang H, Dastani HB, Melero I (2017) Nivolumab in patients with advanced hepatocellular carcinoma (CheckMate 040): an open-label, non-comparative, phase 1/2 dose escalation and expansion trial. *The Lancet* 389:2492-2502. [https://doi.org/10.1016/s0140-6736\(17\)31046-2](https://doi.org/10.1016/s0140-6736(17)31046-2)
15. Fossey SC, Kuroda S, Price JA, Pendleton JK, Freedman BI, Bowden DW (2000) Identification and characterization of PRKCBP1, a candidate RACK-like protein. *Mamm Genome* 11:919-925. <https://doi.org/10.1007/s003350010174>
16. Gong F, Chiu LY, Cox B, Aymard F, Clouaire T, Leung JW, Cammarata M, Perez M, Agarwal P, Brodbelt JS, Legube G, Miller KM (2015) Screen identifies bromodomain protein ZMYND8 in chromatin recognition of transcription-associated DNA damage that promotes homologous recombination. *Genes Dev* 29:197-211. <https://doi.org/10.1101/gad.252189.114>
17. Gong F, Clouaire T, Aguirrebengoa M, Legube G, Miller KM (2017) Histone demethylase KDM5A regulates the ZMYND8-NuRD chromatin remodeler to promote DNA repair. *J Cell Biol* 216:1959-1974. <https://doi.org/10.1083/jcb.201611135>
18. Gong F, Miller KM (2018) Double duty: ZMYND8 in the DNA damage response and cancer. *Cell Cycle* 17:414-420. <https://doi.org/10.1080/15384101.2017.1376150>
19. Ha SY, Choi M, Lee T, Park CK (2016) The Prognostic Role of Mitotic Index in Hepatocellular Carcinoma Patients after Curative Hepatectomy. *Cancer Res Treat* 48:180-189. <https://doi.org/10.4143/crt.2014.321>
20. Hoshida Y, Villanueva A, Kobayashi M, Peix J, Chiang DY, Camargo A, Gupta S, Moore J, Wrobel MJ, Lerner J, Reich M, Chan JA, Glickman JN, Ikeda K, Hashimoto M, Watanabe G, Daidone MG, Roayaie S, Schwartz M, Thung S, Salvesen HB, Gabriel S, Mazzaferro V, Bruix J, Friedman SL, Kumada H, Llovet JM, Golub TR (2008) Gene expression in fixed tissues and outcome in hepatocellular carcinoma. *N Engl J Med* 359:1995-2004. <https://doi.org/10.1056/NEJMoa0804525>
21. Imamura H, Matsuyama Y, Tanaka E, Ohkubo T, Hasegawa K, Miyagawa S, Sugawara Y, Minagawa M, Takayama T, Kawasaki S, Makuuchi M (2003) Risk factors contributing to early and late phase intrahepatic recurrence of hepatocellular carcinoma after hepatectomy. *J Hepatol* 38:200-207
22. Inagaki Y, Shiraki K, Sugimoto K, Yada T, Tameda M, Ogura S, Yamamoto N, Takei Y, Ito M (2016) Epigenetic regulation of proliferation and invasion in hepatocellular carcinoma cells by CBP/p300 histone acetyltransferase activity. *Int J Oncol* 48:533-540. <https://doi.org/10.3892/ijo.2015.3288>
23. Kudo M, Finn RS, Qin S, Han K-H, Ikeda K, Piscaglia F, Baron A, Park J-W, Han G, Jassem J, Blanc JF, Vogel A, Komov D, Evans TRJ, Lopez C, Dutcus C, Guo M, Saito K, Kraljevic S, Tamai T, Ren M, Cheng A-L (2018) Lenvatinib versus sorafenib in first-line treatment

- of patients with unresectable hepatocellular carcinoma: a randomised phase 3 non-inferiority trial. *The Lancet* 391:1163-1173. [https://doi.org/10.1016/s0140-6736\(18\)30207-1](https://doi.org/10.1016/s0140-6736(18)30207-1)
24. Kuroyanagi J, Shimada Y, Zhang B, Ariyoshi M, Umemoto N, Nishimura Y, Tanaka T (2014) Zinc finger MYND-type containing 8 promotes tumour angiogenesis via induction of vascular endothelial growth factor-A expression. *FEBS Lett* 588:3409-3416. <https://doi.org/10.1016/j.febslet.2014.07.033>
25. Li M, Luo RZ, Chen JW, Cao Y, Lu JB, He JH, Wu QL, Cai MY (2011) High expression of transcriptional coactivator p300 correlates with aggressive features and poor prognosis of hepatocellular carcinoma. *J Transl Med* 9:5. <https://doi.org/10.1186/1479-5876-9-5>
26. Li N, Li Y, Lv J, Zheng X, Wen H, Shen H, Zhu G, Chen TY, Dhar SS, Kan PY, Wang Z, Shiekhattar R, Shi X, Lan F, Chen K, Li W, Li H, Lee MG (2016) ZMYND8 Reads the Dual Histone Mark H3K4me1-H3K14ac to Antagonize the Expression of Metastasis-Linked Genes. *Mol Cell* 63:470-484. <https://doi.org/10.1016/j.molcel.2016.06.035>
27. Lim HY, Sohn I, Deng S, Lee J, Jung SH, Mao M, Xu J, Wang K, Shi S, Joh JW, Choi YL, Park CK (2013) Prediction of disease-free survival in hepatocellular carcinoma by gene expression profiling. *Ann Surg Oncol* 20:3747-3753. <https://doi.org/10.1245/s10434-013-3070-y>
28. Liver Cancer Study Group of Japan (2003) *The general rules for the clinical and pathological study of primary liver cancer*, 2nd edn, Tokyo, Kanahara
29. Llovet JM, Bru C, Bruix J (1999) Prognosis of hepatocellular carcinoma: the BCLC staging classification. *Semin Liver Dis* 19:329-338. <https://doi.org/10.1055/s-2007-1007122>
30. Ma L, Li G, Zhu H, Dong X, Zhao D, Jiang X, Li J, Qiao H, Ni S, Sun X (2014) 2-Methoxyestradiol synergizes with sorafenib to suppress hepatocellular carcinoma by simultaneously dysregulating hypoxia-inducible factor-1 and -2. *Cancer Lett* 355:96-105. <https://doi.org/10.1016/j.canlet.2014.09.011>
31. Mootha VK, Lindgren CM, Eriksson KF, Subramanian A, Sihag S, Lehar J, Puigserver P, Carlsson E, Ridderstrale M, Laurila E, Houstis N, Daly MJ, Patterson N, Mesirov JP, Golub TR, Tamayo P, Spiegelman B, Lander ES, Hirschhorn JN, Altshuler D, Groop LC (2003) PGC-1alpha-responsive genes involved in oxidative phosphorylation are coordinately downregulated in human diabetes. *Nat Genet* 34:267-273. <https://doi.org/10.1038/ng1180>
32. Portolani N, Coniglio A, Ghidoni S, Giovanelli M, Benetti A, Tiberio GA, Giulini SM (2006) Early and late recurrence after liver resection for hepatocellular carcinoma: prognostic and therapeutic implications. *Ann Surg* 243:229-235. <https://doi.org/10.1097/01.sla.0000197706.21803.a1>
33. Qin LX, Tang ZY (2004) Recent progress in predictive biomarkers for metastatic recurrence of human hepatocellular carcinoma: a review of the literature. *J Cancer Res Clin Oncol* 130:497-513. <https://doi.org/10.1007/s00432-004-0572-9>
34. Remmele W, Stegner HE (1987) [Recommendation for uniform definition of an immunoreactive score (IRS) for immunohistochemical estrogen receptor detection (ER-ICA) in breast cancer tissue]. *Pathologe* 8:138-140
35. Shen H, Xu W, Guo R, Rong B, Gu L, Wang Z, He C, Zheng L, Hu X, Hu Z, Shao ZM, Yang P, Wu F, Shi YG, Shi Y, Lan F (2016) Suppression of Enhancer Overactivation by a RACK7-Histone Demethylase Complex. *Cell* 165:331-342. <https://doi.org/10.1016/j.cell.2016.02.064>
36. Sherman M (2008) Recurrence of hepatocellular carcinoma. *N Engl J Med* 359:2045-2047. <https://doi.org/10.1056/NEJMe0807581>
37. Shimada M, Hamatsu T, Yamashita Y, Rikimaru T, Taguchi K, Utsunomiya T, Shirabe K, Sugimachi K (2001) Characteristics of multicentric hepatocellular carcinomas: comparison with intrahepatic metastasis. *World J Surg* 25:991-995
38. Subramanian A, Tamayo P, Mootha VK, Mukherjee S, Ebert BL, Gillette MA, Paulovich A, Pomeroy SL, Golub TR, Lander ES, Mesirov JP (2005) Gene set enrichment analysis: a knowledge-based approach for interpreting genome-wide expression profiles. *Proc Natl Acad Sci U S A* 102:15545-15550. <https://doi.org/10.1073/pnas.0506580102>
39. Tang Z, Li C, Kang B, Gao G, Li C, Zhang Z (2017) GEPIA: a web server for cancer and normal gene expression profiling and interactive analyses. *Nucleic Acids Res* 45:W98-W102. <https://doi.org/10.1093/nar/gkx247>
40. Wang Y, Luo M, Chen Y, Wang Y, Zhang B, Ren Z, Bao L, Wang Y, Wang JE, Fu YX, Luo W, Wang Y (2020) ZMYND8 expression in breast cancer cells blocks T-lymphocyte surveillance to promote tumor growth. *Cancer Res*. <https://doi.org/10.1158/0008-5472.CAN-20-1710>
41. Xiang ZL, Zeng ZC, Fan J, Tang ZY, He J, Zeng HY, Chang JY (2012) The expression of HIF-1alpha in primary hepatocellular carcinoma and its correlation with radiotherapy response and clinical outcome. *Mol Biol Rep* 39:2021-2029. <https://doi.org/10.1007/s11033-011-0949-1>

42. Yeo S-Y, Lee K-W, Shin D, An S, Cho K-H, Kim S-H (2018) A positive feedback loop bi-stably activates fibroblasts. *Nature communications* 9:1-16
43. Yu H, Jiang Y, Liu L, Shan W, Chu X, Yang Z, Yang ZQ (2017) Integrative genomic and transcriptomic analysis for pinpointing recurrent alterations of plant homeodomain genes and their clinical significance in breast cancer. *Oncotarget* 8:13099-13115. <https://doi.org/10.18632/oncotarget.14402>
44. Zhu AX, Finn RS, Edeline J, Cattani S, Ogasawara S, Palmer D, Verslype C, Zagonel V, Fartoux L, Vogel A, Sarker D, Verset G, Chan SL, Knox J, Daniele B, Webber AL, Ebbinghaus SW, Ma J, Siegel AB, Cheng A-L, Kudo M, Alistar A, Asselah J, Blanc J-F, Borbath I, Cannon T, Chung K, Cohn A, Cosgrove DP, Damjanov N, Gupta M, Karino Y, Karwal M, Kaubisch A, Kelley R, Van Laethem J-L, Larson T, Lee J, Li D, Manhas A, Manji GA, Numata K, Parsons B, Paulson AS, Pinto C, Ramirez R, Ratnam S, Rizell M, Rosmorduc O, Sada Y, Sasaki Y, Stal PI, Strasser S, Trojan J, Vaccaro G, Van Vlierberghe H, Weiss A, Weiss K-H, Yamashita T (2018) Pembrolizumab in patients with advanced hepatocellular carcinoma previously treated with sorafenib (KEYNOTE-224): a non-randomised, open-label phase 2 trial. *The Lancet Oncology* 19:940-952. [https://doi.org/10.1016/s1470-2045\(18\)30351-6](https://doi.org/10.1016/s1470-2045(18)30351-6)

Figures

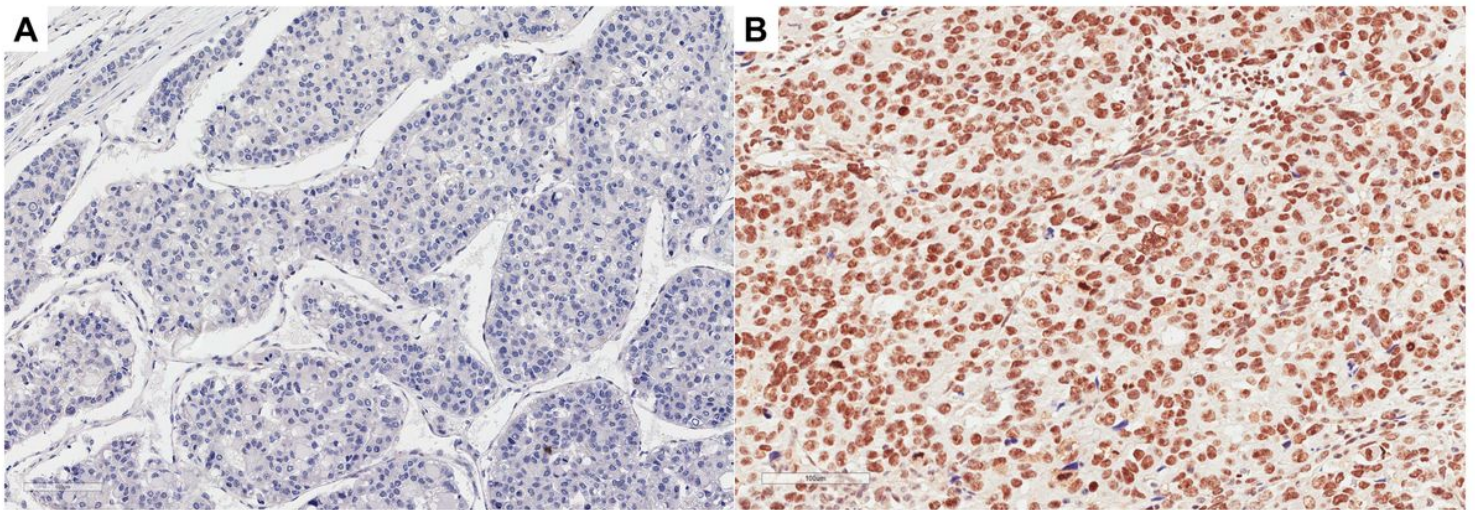


Figure 1

Representation of ZMYND8 expression in hepatocellular carcinoma by immunohistochemistry. (A) Tumor cells show negative staining for ZMYND8. (B) Tumor cells show nuclear staining for ZMYND8.

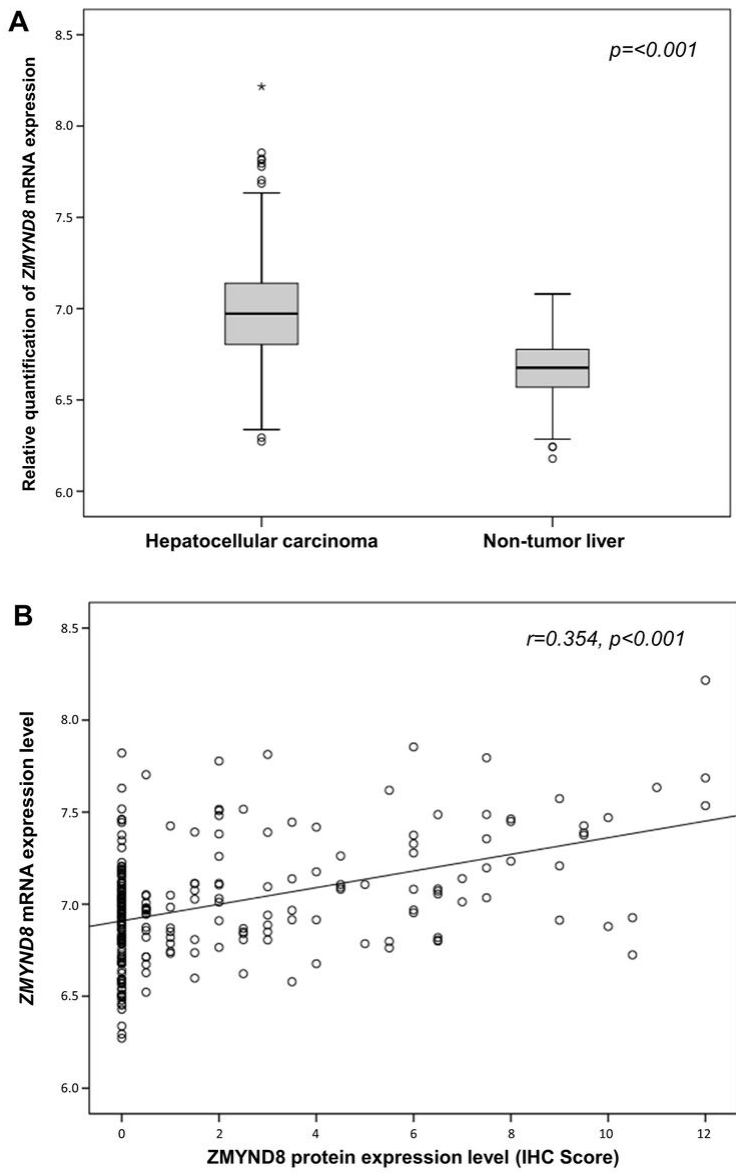


Figure 2

The relative quantification of ZMYND8 mRNA expression in hepatocellular carcinoma and background non-tumor liver (A), and the relationship between ZMYND8 protein and ZMYND8 mRNA expression (B). IHC, immunohistochemistry

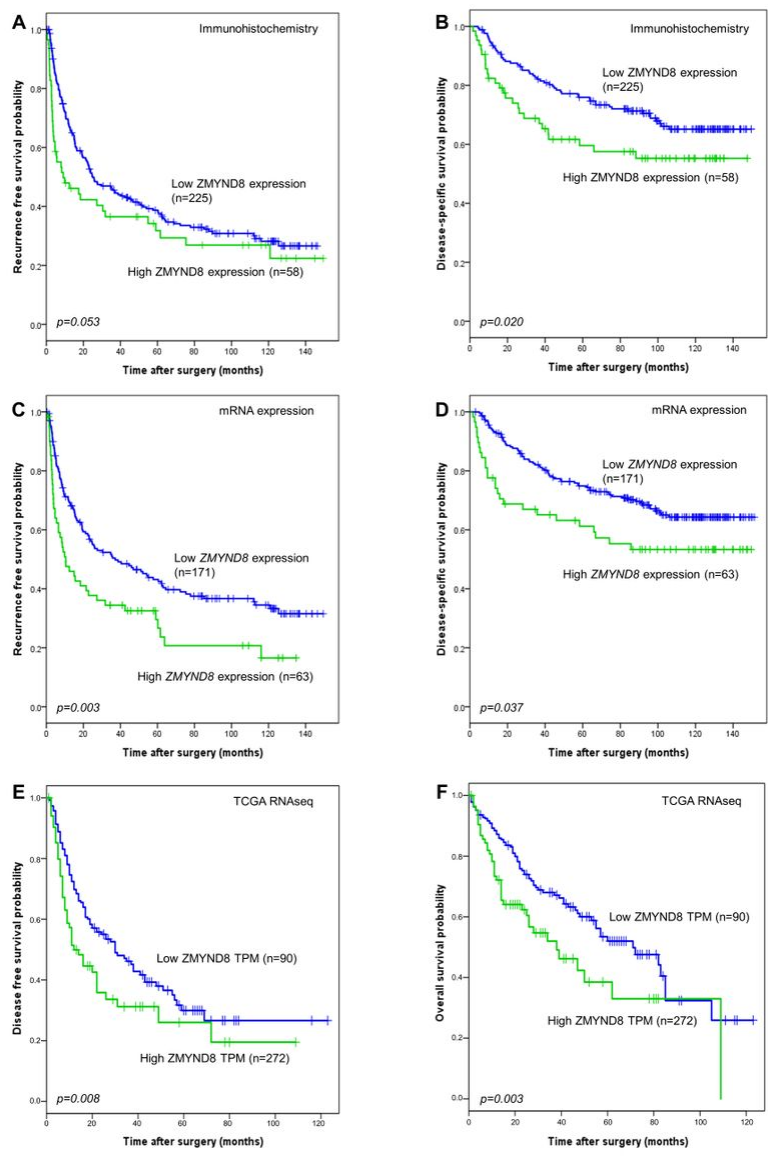


Figure 3

Kaplan-Meier survival curves according to ZMYND8 expression. (A-B) Survival curves according to ZMYND8 protein expression by immunohistochemistry (C-D) Survival curves according to ZMYND8 mRNA expression by microarray gene expression data (E-F) Survival curves according to ZMYND8 mRNA expression by TCGA RNAseq data. TCGA, The Cancer Genome Atlas

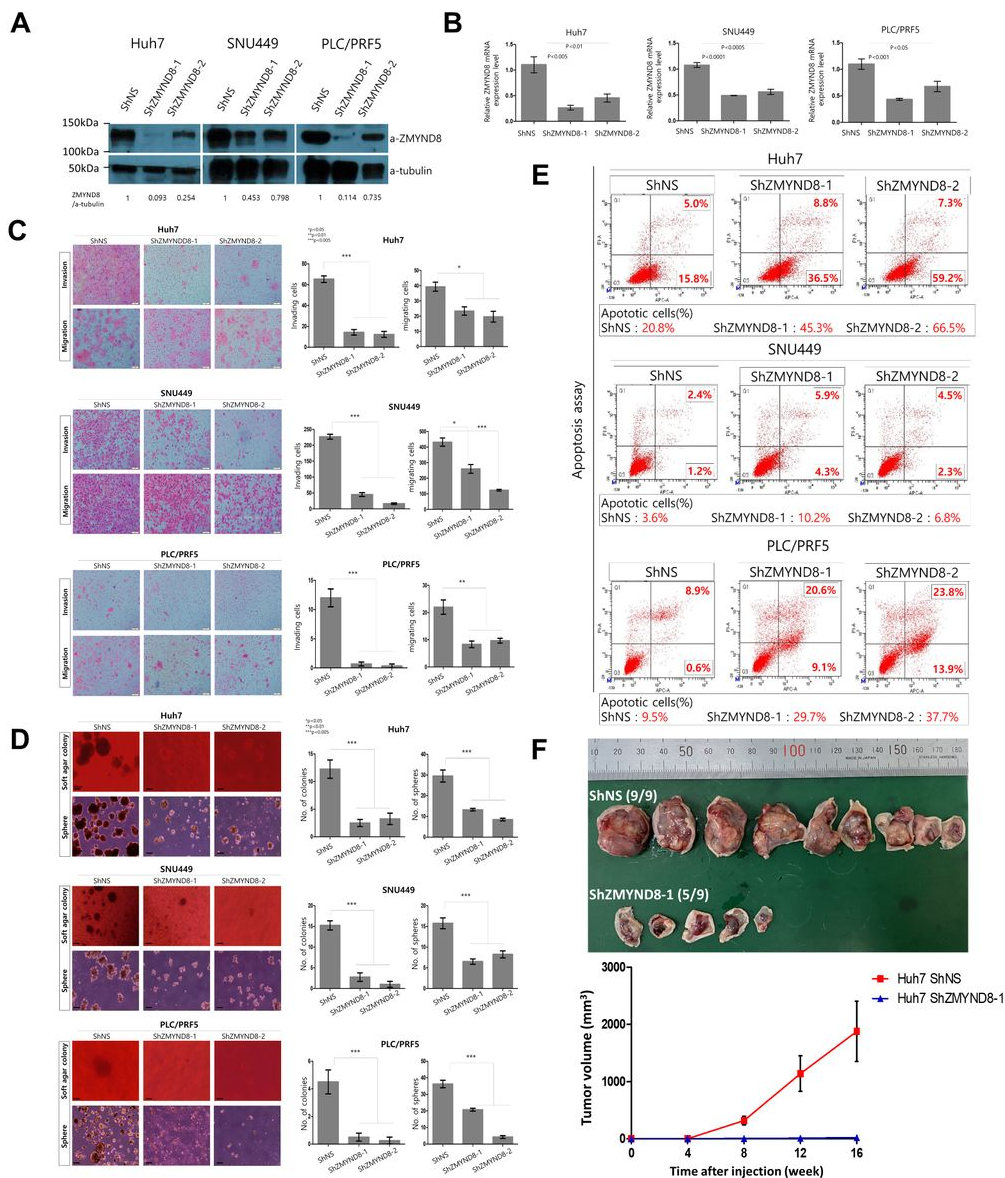


Figure 4

Downregulation of ZMYND8 expression by ShRNA was confirmed at protein (A) and mRNA level (B). Knockdown of ZMYND8 resulted in significantly reduced migration, invasion (C), sphere formation, colony formation (D), and increased apoptosis of HCC cells (E). Inhibition of tumor growth was observed in a ZMYND8 knockdown HCC Xenograft in nude mice (F).

Supplementary Files

This is a list of supplementary files associated with this preprint. Click to download.

- [SupplementaryTable1.pdf](#)